Journal of Cellular Biochemistry 25:73–86 (1984)

Characterization of Thermotropic Structural Transitions of the Erythrocyte Membrane: A Biochemical and Electron-Paramagnetic Resonance Approach

Maurizio Minetti, Marina Ceccarini, and Anna Maria M. Di Stasi

Department of Cell Biology, Istituto Superiore di Sanità, 00161 Rome, Italy

The relationship between membrane structural properties and functions has been generally inferred from observed thermotropic phenomena. By the use of 16-dinyloxyl stearic acid spin probe we investigated the red blood cell membrane components involved in three characteristic thermotropic structural transitions occurring at 8, 20, and 40°C. The transition at 8°C is removed by chymotrypsin treatment at the cytoplasmic membrane layer. The 20°C phase transition is unmodified after chymotrypsin treatment and occurs at 15°C after complete proteolysis of intramembrane chymotrypsin-insensitive peptides. Liposomes from the total lipid extract of RBC show only one thermotropic transition at 15°C. The 40°C phase transition is absent in vesicles free of skeletal proteins, in vesicles obtained after RBC storage, and in low-ionic-strength resealed ghosts. Transitions at 8°C and 40°C appear to be due to the interactions of cytoplasmic exposed proteins with membrane, whereas the 20°C transition is intrinsic to the lipid component.

Key words: spin-labeling of erythrocyte membrane, membrane structural transitions, protein-lipid interactions, membrane organization

A functionally specialized mosaic distribution of membrane components seems to be a more realistic model than the generally fluid bilayer concept of membrane (see [1] and references reported therein). In this respect it is crucial to show a relationship between structural lipid properties and membrane functions.

In the case of red blood cells (RBC), the presence of a domain-based structure is under discussion. Preliminary evidence for the presence of domains can be deduced by the asymmetric and nonrandom distribution of both proteins and lipids [2–9], by the clustering of charged amino phospholipids [9] and, at least below 5°C, by the intramembrane particle aggregation observed without the removal of skeletal proteins

Abbreviations used: 16-DSA, 2-(14-carboxy-tetradecyl)-2-ethyl-4,4-dimethyl-3-oxazoli-dinyloxyl; EPR, electron paramagnetic resonance; PBS, phosphate-buffered saline.

Received September 21, 1983; accepted February 7, 1984.

[10]. The possibility of relating structural properties of membrane components and membrane functions is suggested by the presence of structural transitions at temperatures similar to those of some thermotropic biological phenomena [10–14].

The occurrence of structural transitions of RBC membrane components has been described by using a variety of physicochemical methods [10–29]. This notwithstanding, the structural changes involved in these transitions is not well understood. Data obtained by Verma and Wallach [18,20,30] with Raman spectroscopy suggest that thermotropic transitions in the 0–37°C range are due to gel-liquid phase transitions of lipids (or of protein-lipid domains), whereas transitions at higher temperatures could be due to protein thermal denaturation. The existence of gel-liquid phase transitions in RBC membrane above 0°C, however, is controversial [31]. The presence of cooperative gel-liquid phase transitions in extended area of RBC membrane is unlikely in view of the high cholesterol content and, in addition, a random distribution of the sterol would abolish any cooperative phase transition [7].

Spin-labeled stearic acids have been shown to be convenient to study RBC structural transitions [14,15,22,25,27–29]. The main question that arises from these studies is the meaning of the thermotropic transitions detected by this technique. In this paper we address this question by looking at membrane components possibly involved in three thermotropic changes detected by a 16-dinyloxyl stearic acid (16-DSA) spin probe as modifications in its freedom of motion. We have reported a preliminary characterization of the thermotropic transitions by using modified RBC membrane preparations. As a result of this study two thermotropic transitions at 8°C and 40°C appear to be due to the presence of cytoplasmic exposed proteins, and the other transition at 20°C appears to be due to lipids.

EXPERIMENTAL PROCEDURE

EPR Measurements

Human RBC were washed three times in phosphate-buffered saline, PBS (150 mM NaCl, 5 mM sodium phosphate, pH 7.8), and the buffy coat accurately removed each time. The 16-DSA (Syva, Palo Alto, CA) spin probe was dissolved in absolute ethanol at the concentration of 10 mM and the solvent was evaporated under a nitrogen stream. To 10 μg of the dried probe, an amount of RBC corresponding to 1 mg of membrane proteins (or lipids) was added. Incorporation of the probe into RBC membranes was achieved by incubation at 37°C for 1 hr. The EPR spectra were recorded on a Varian E-4 spectrometer (Milan, Italy) equipped with a variable temperature accessory. Temperature was monitored, with an accuracy of $\pm$ 0.1°C, by a digital thermometer set above the cavity. At each temperature four spectra were recorded and the average value of the peak heights used for calculations.

EPR Data Analysis

After empirical evaluation of break points in the plot of log (h_0/h_{-1}) vs 1/T, the regression lines interpolating the experimental data were estimated with the least-squares method. The analysis of variance on the regression coefficients was also performed, showing highly significant differences between them. In detail, all the regression coefficients (slopes) had the 95% confidence limits not overlapping each other. Similar results were obtained by changing the break points (no more than $\pm$

1.5°C for each break) and the corresponding slopes resulted coincident within their 95% confidence limits.

The simultaneous estimation of break points and regression parameters was performed with the D-506 computer program (MINUIT) from CERN Computer Library. The results confirmed the previous estimations: the break point resulted coincident with ± 1.5°C, and the regression coefficients within the previous estimated confidence limits.

Proteolytic Treatments

Washed RBC were rapidly lysed at 0°C in 5 mM sodium phosphate, pH 7.8, containing 1 mg/ml of proteolytic enzymes. Papain (Worthington, Freehold, NJ) was activated with 0.1 mM cysteine. The cell/buffer ratio was 1:10 (v/v). To reseal RBC, KCl was added to reach a final concentration of 145 mM. After 1 hr incubation at 37°C the cells were washed three times in PBS by 5 min centrifugations at 48,000g. Phenylmethyl-sulfonyl fluoride (1 mM) (Sigma, St Louis, MO) was added to stop proteolytic digestion with chymotrypsin (Boehringer, West Germany). Treatment with thermolysine (Boehringer, West Germany) was carried out as for the other enzymes except that Tris-HCl buffer, containing 10 mM $CaCl_2$ was used instead of phosphate buffer.

RBC Storage and Vesicle Separation

Washed RBC were incubated 48 hr at 37°C in 10 mM Tris, 150 mM NaCl, 1 mM $CaCl_2$, pH 7.8, in cell/buffer ratio of 1:10 (v/v). Penicillin-streptomycin solution (GIBCO, Scotland) at a concentration 1,000 U/ml was added during the incubation period to avoid microbial growth. The cells were then centrifuged 10 min at 2,000g. Supernatant, containing released vesicles, was centrifuged for 2 hr at 48,000g. The pellet was resuspended in 4 ml of 10 mM Tris, 150 mM NaCl buffer, and layered upon 6 ml of Lymphoprep (Nyegaard, Norway). The sample was then centrifuged 20 min at 2,500g and the interface between buffer and Lymphoprep, containing vesicles, was filtered twice on 1-μm cellulose membrane filter (BioRad, Richmond, CA). Microscopic observation of samples showed the presence of small vesicles and the absence of residual RBC or ghosts. Chymotrypsin treatment was carried out by suspending vesicles in PBS containing 1 mg/ml chymotrypsin. After three cycles of freezing and thawing, to allow enzyme penetration, the samples were incubated for 1 hr at 37°C.

Alkali-Stripped Ghosts and Multilamellar Liposomes

Erythrocytes were lysed in 5 mM sodium phosphate, pH 7.8, according to Steck and Kant [32]. Stripped ghosts were obtained by a short exposure at 0°C of lysed ghosts to pH 12 according to Gerritsen et al [33]. Multilamellar liposomes were prepared by vortexing in PBS at 37°C the total lipid extract of RBC obtained according to Roelofsen et al [34].

Sodium Dodecyl Sulfate Gel Electrophoresis

RBC membrane proteins were analyzed by sodium dodecyl sulfate polyacrylamide gel electrophoresis carried out according to Laemmli [35], using 6% polyacrylamide slab gel for membrane proteins, and 17% polyacrylamide slab gel for peptide

analysis of protease-treated RBC. Before gel electrophoresis, proteases were inactivated by 5 min incubation at 100°C. Gels were stained with Coomassie Blue and electrophoretic profiles were recorded with a Zeiss Chromatographic Spectrometer PMQ 3 (Zeiss, Oberkochen, West Germany).

RESULTS

Analysis of EPR Spectra of Intact RBC

The 16 DSA spin probe explores the hydrophobic core of the membrane and has been successfully utilized to study RBC thermotropic properties [14,15,22,25,27–29]. This label is preferentially incorporated into the membrane and we observed that the label detectable in the supernatant of the cell hemolysate was shaped as expected for a free label and was only a small percentage ($<1\%$) of the membrane-bound label.

Typical spectra at 37°C and 0°C of 16-DSA in RBC membrane are shown in Figure 1. These spectra are characteristic of a probe experiencing anisotropic motions within a biological membrane with an apparent correlation time, τ_c, at 37°C of the order of 1.5×10^{-9} sec. A precise estimate of the label motion, shown by the spectra of Figure 1, would require a detailed numerical separation by computer simulation of different contributions to the peaks [36].

In any event, our purpose here is to measure relative spectra changes of the label into a membrane as a function of temperature. In RBC membrane the use of correlation time measured by simplified equation [36] may be incorrect in view of membrane anisotropy and uncertainty in probe localization(s). Therefore τ_c measurements are to be considered parameters indicative of relative changes in the amplitude and/or rate of spin label motions, but do not necessarily imply a change in correlation time. We anaylzed the RBC spectra by using the empirical parameter log (h_0/h_{-1}) instead of the apparent τ_c. The two parameters utilize the same spectral value (ie, h_0 and h_1 ratio) except that τ_c contains also the width of the central line, w_0. In intact RBC w_0 is linear up to 37–40°C and thereafter a more rapid narrowing of the line is observed. A similar discontinuous narrowing was not observed in membranes lacking skeletal proteins. Thus for the experiments reported, the use of log (h_0/h_{-1}) or τ_c produces similar thermotropic breaks.

The plot of log (h_0/h_{-1}) against the reciprocal of the temperature for both intact RBC and RBC ghosts are reported in Figure 2. The discontinuities can be described as break points of the regression lines presented. Thermotropic breaks are present at 8, 20, and 40° $\pm$ 1.5°C. EPR studies reported previously [14,22,25,27,37] showed the presence in the 0–30°C range of only one thermotropic break apparently overlooking one of the low temperature breaks. A more accurate analysis revealed the presence of two thermotropic breaks in the 0–30°C range. These breaks are thought to reflect structural changes in RBC membranes at the level of proteins, lipids, or both. 16-DSA detects these membrane structural changes as modifications in the freedom of motion, but the physical significance of these changes is not well understood. Thus, under the limitations of this technique, we call these breaks thermotropic structural transitions.

Proteolytic Treatment of RBC

In order to identify membrane components involved in the thermotropic transitions detected by 16-DSA, the following three membrane models were derived from

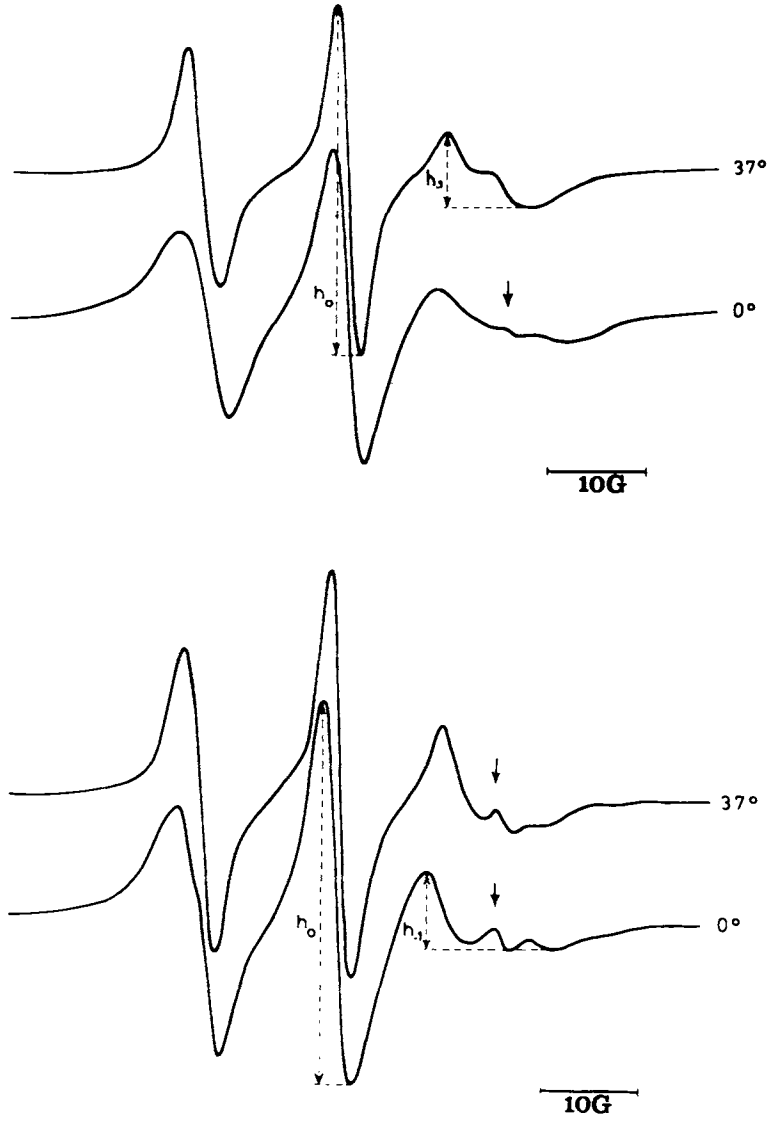

Fig. 1. Typical 16-DSA spectra at 37°C and 0°C of RBC (upper curves) and chymotrypsin-digested RBC (lower curves). The assignment of lines h_0 and h_{-1} is shown. The arrow indicates the position of free label. Experimental errors usually decrease with increasing temperature; typical values of log (h_0/h_{-1}) ± SEM for control RBC are: 0.687 ± 0.04 at 37°C and 0.785 ± 0.08 at 0°C. Break temperatures were determined by computer analysis.

RBC: chymotrypsin-digested RBC without hemolytic shock; chymotrypsin-digested RBC after a hemolytic shock to allow enzyme penetration inside the cell (hereafter indicated as chymotrypsin-digested RBC); and papain-digested RBC after a hemolytic shock (hereafter indicated as papain-digested RBC).

RBC digested externally by chymotrypsin did not show changes in the plot of log (h_0/h_{-1}) vs 1/T (data not shown), thus suggesting that externally exposed proteins are not relevant in the EPR thermotropic breaks.

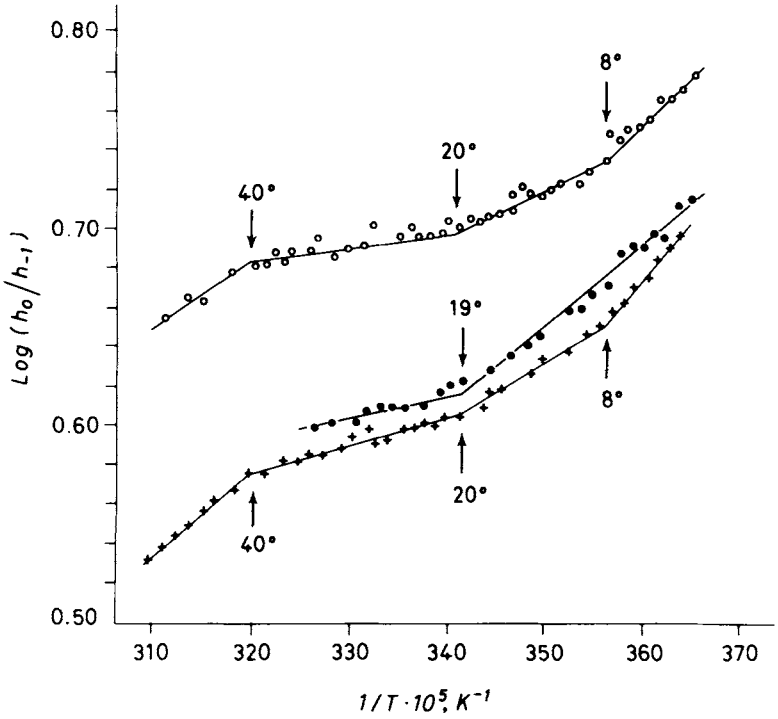

Fig. 2. The plot of log (h_0/h_{-1}) vs 1/T for RBC (○—○); for chymotrypsin-digested RBC (●—●) and for resealed RBC ghosts. (+—+) Points are average values of four spectra.

The spectra of chymotrypsin-digested RBC are reported in Figure 1. It can be observed that on the h_{-1} line a distinct component is superimposed. This additional signal coincides with the position of free label but is not removed after cell washings. It may be due to a label partition into the cell cytoplasm and/or in a polar domain that, for unknown reasons, appears to be more represented after proteolysis. In untreated RBC this additional signal seems to be present but at a very low extent (see the arrow in Fig. 1) In chymotrypsin-digested RBC, but not in control RBC, the presence of this distinct component on line h_{-1} modifies the spectra above 35°C so that spectral parameters were difficult to measure (Fig. 1). The plot of log (h_0/h_{-1}) in the 0–35°C temperature range for chymotrypsin-digested RBC is reported in Figure 2. It can be observed that after this treatment the phase transition at 20°C is virtually unmodified (Fig. 2). The 20°C phase transition thus appears to be due to membrane components inaccessible and/or insensitive to the enzyme. It is obvious that the disappearance of a phase transition may be due to the removal of the component(s) directly or indirectly involved in the structural transition or to the fall of the break point out of the temperature range explored (ie, 0–50°C). On the other hand RBC lipids undergo a quasi-cooperative phase transition of bulk lipids below 0°C [20,31], and, above 50°C, thermal denaturation of proteins and membrane fragmentation occurs [38].

As reported by Weinstein et al [39] chymotrypsin treatment of unsealed RBC membrane causes extensive proteolysis of the major membrane proteins (ie, bands 1,

2, 2.1, 3, 4.1, 4.2, 4.5, and 5; nomenclature of bands according to Steck [40]). Although this treatment removes about 70% of membrane proteins, these membranes submitted to freeze-fracture presented, at the protoplasmic fracture face, the so-called intramembrane particles morphologically intact [39]. Sodium dodecyl sulfate gel electrophoresis of peptides in chymotrypsin-digested RBC reveals, in fact, the presence of discrete bands at molecular weight between 30,000 and 50,000 (Fig. 3).

To study the role of these residual polypeptides on thermotropic breaks, RBC were digested, after a hemolytic shock, with thermolysine or papain. Figure 3 shows that papain is the most effective enzyme in digesting RBC membrane proteins. Papain-digested RBC, in fact, do not contain discrete peptides after sodium dodecyl sulfate polyacrylamide gel electrophoresis (Fig. 3). The plot of log (h_0/h_{-t}) vs 1/T for these membranes shows only one transition at 16°C (Fig. 4). This suggests that papain digestion of the polypeptides responsible for intramembrane particles, causes a lowering of the transition from 20°C to 16°C. An identical result was obtained after Triton X-100 solubilization of chymotrypsin-digested RBC, papain treatment, and detergent removal by Bio-Beads SM-2 (data not shown). This residual transition may be due, therefore, to membrane lipids. To confirm these results, multilamellar lipo-

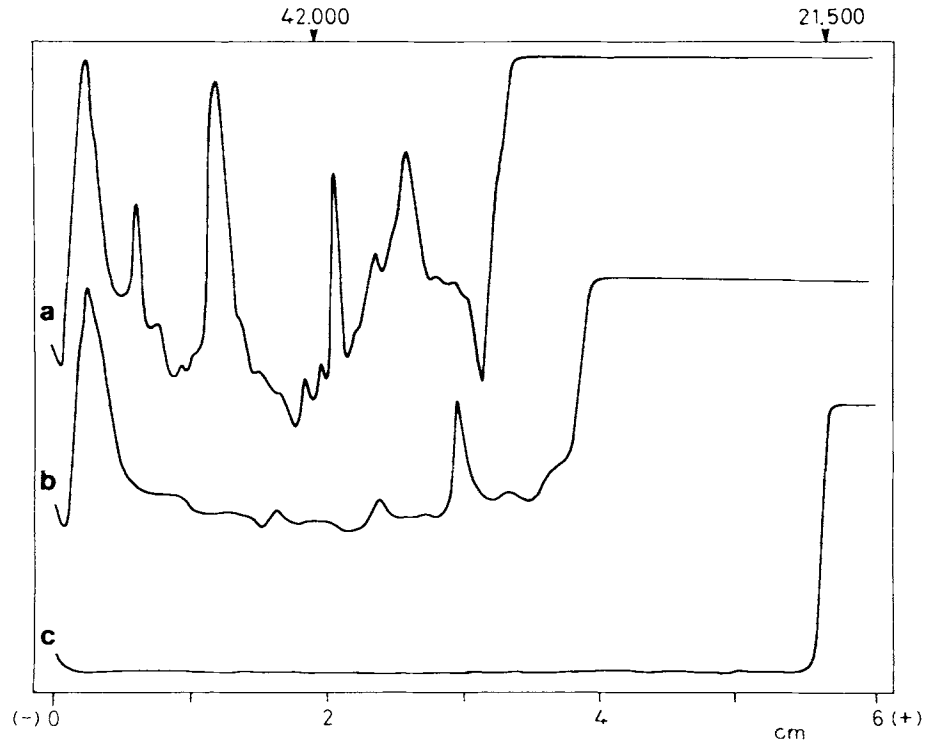

Fig. 3. Electrophoretic profiles of protease-treated RBC. a) Chymotrypsin-digested RBC; b) thermolysine-treated RBC; c) papain-treated RBC. The acrylamide concentration was 17%. Gels were stained with Coomassie Blue. Arrows indicate the position of molecular weight standards (muscle actin 42,000; soybean trypsin inhibitor 21,500). The same membrane amount (300 μg, dry weight) was applied to each well. The high absorbance at the end of electrophoretic profiles is due to heterogeneous breakdown products.

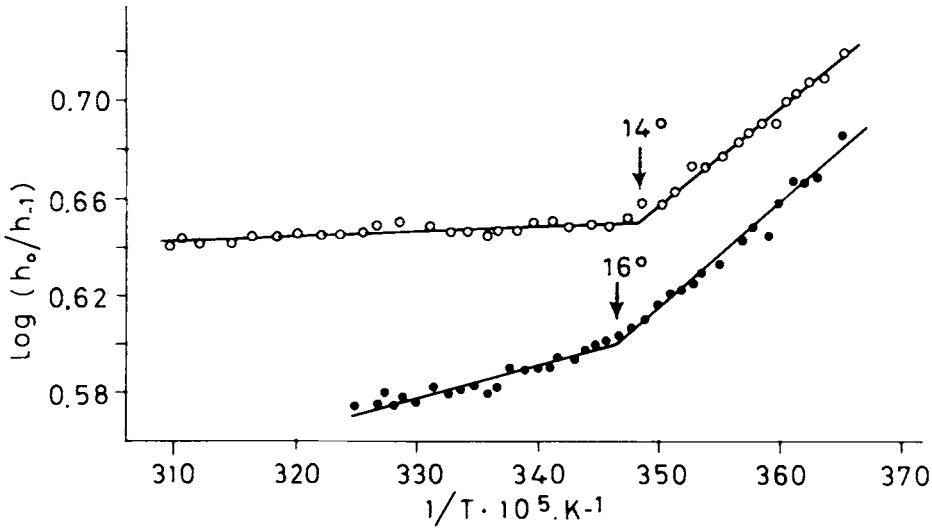

Fig. 4. The plot of log (h_0/h_{-1}) vs 1/T for papain-digested RBC (●—●) and for multilamellar liposomes from total RBC lipids (○—○).

somes were prepared from total lipid extract of RBC ghosts. The plot of log (h_0/h_{-1}) for these liposomes shows a break centered around 14°C (Fig. 4).

Vesicles Obtained From RBC After Storage and Cytoskeletal Extraction

RBC depleted of ATP for more than 20 hr are known to release spectrin-free vesicles [41–43]. RBC kept at 37°C for 48 hr released vesicular material that, after separation and purification, shows the electrophoretic pattern reported in Figure 5. As previously reported by Lutz [44], the most evident difference in the electrophoretic pattern between these vesicles and control ghosts is found at the level of skeletal proteins (Fig. 5). The electrophoretic profile of vesicles released from RBC is similar to that obtained from alkali-stripped ghosts (Fig. 5). This last treatment is known to produce skeletal protein extraction [33,45] (Fig. 5). The plot of log (h_0/h_{-1}) against the reciprocal of temperature for vesicles obtained after RBC storage and for alkali-stripped ghosts is reported in Figure 6. Both these membranes show two clear breaks at about 8°C and 20°C.

To test the effects of chymotrypsin on thermotropic structural transitions of vesicles obtained after RBC storage, these membranes were treated with chymotrypsin and then freeze-thawed to allow enzyme penetration. As for RBC, chymotrypsin effaces the 8°C transition of vesicles but the 20°C transition is maintained (Fig. 6).

If one analyses the plot of log (h_0/h_{-1}) of vesicles obtained after RBC storage or after alkali treatment, the 40°C transition is absent (Fig. 6). We observe that the lack of skeletal proteins (Fig. 5) in vesicles obtained from RBC is concomitant with the lack of 40°C transition (Fig. 6). The hypothesis that skeletal proteins are responsible for the 40°C transition appears to be plausible. Data reported in Figure 7 of the accompanying paper [15] on glutaraldehyde-treated RBC are in accordance with this hypothesis. Glutaraldehyde is an hydrophilic cross-linking agent known to react preferentially with skeletal proteins [46]. The plot of log (h_0/h_{-1}) for 0.4 mM

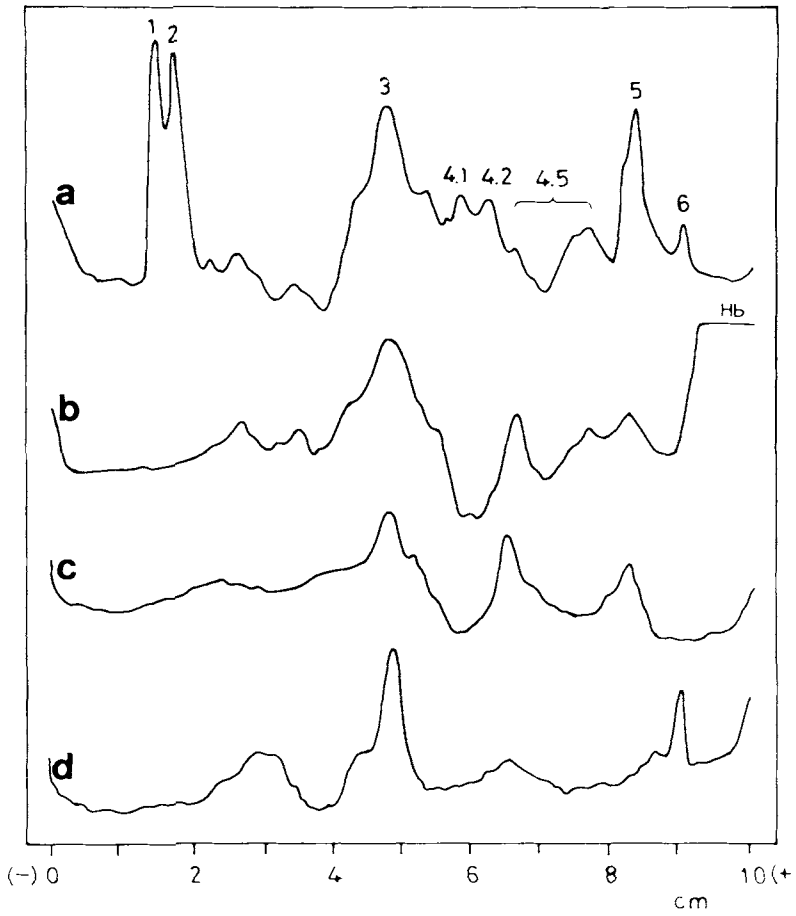

Fig. 5. Electrophoretic profiles of ghost proteins and various RBC membrane preparations. a) Control ghosts; b) vesicles obtained after RBC storage; c) alkali-stripped ghosts; d) 0.4 mM glutaraldehyde-treated RBC. The acrylamide concentration was 6%. Gels were stained with Coomassie Blue. The same membrane amount (50–80 μg, dry weight) was applied to each well. Nomenclature of bands according to Steck [40]. Hb = hemoglobin.

glutaraldehyde-treated RBC shows only one break at 18°C whereas the 40°C break is not observed. The disappearance of the 40°C transition may be related to the cross-linking of skeletal proteins. The formation of high-molecular-weight complexes produces, in fact, the lack of skeletal proteins in the electrophoretic profile of these glutaraldehyde-treated RBC (Fig. 5).

Effect of the Low Ionic Strength on the 40°C Thermotropic Transition

The labeling of RBC membrane proteins with the maleimide-analogue sulphydryl spin label has been shown to detect protein thermotropic conformational changes above 40°C [47,48]. A similar conformational change has been observed on purified spectrin preparations, and the conformational change detected by this probe has therefore been attributed to this protein [47].

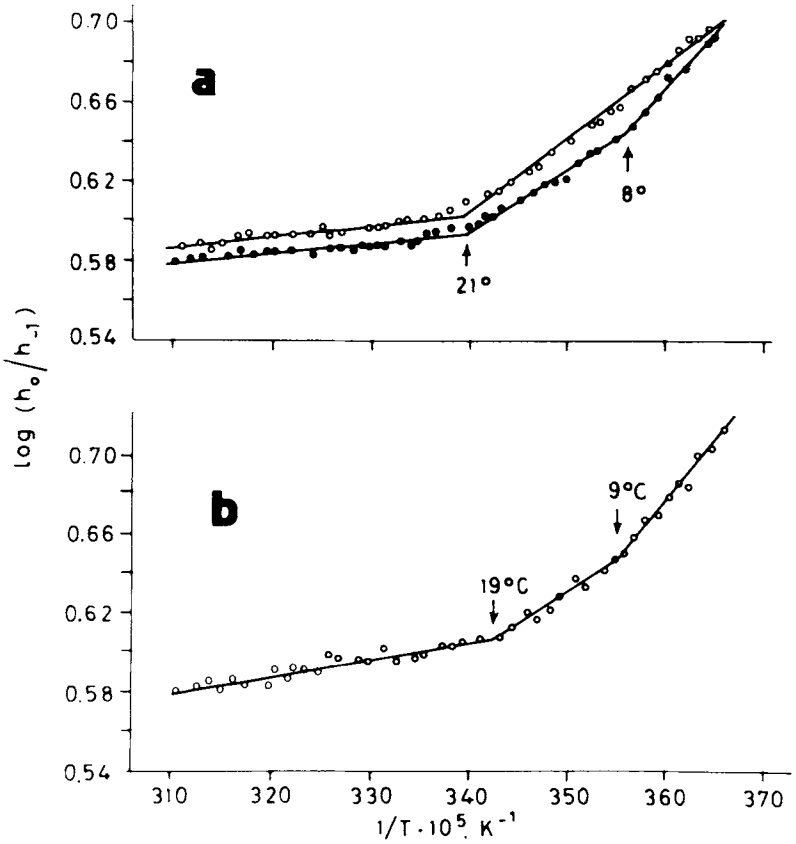

Fig. 6. The plot of log (h_0/h_{-1}) vs 1/T for vesicles obtained after RBC storage and for alkali-stripped ghosts. a) ●—● Vesicles; ○—○, chymotrypsin-digested vesicles; b) alkali-stripped ghosts.

To investigate whether 16-DSA detects the same 40°C conformational transition of maleimide spin label, possibly by a localization of the stearic acid into the same protein pocket, RBC ghosts were resealed at different ionic strengths. NaCl concentrations in the 20–150 mM range are known to slightly modify the maleimide-labeled RBC spectra [49] but do not abolish the thermotropic spectrin conformational change observed above 40°C (our unpublished data). Figure 7 shows the effects of hypotonic salt concentrations on the thermotropic transition of the 16-DSA in the 0–50°C range. The transition, that in control ghosts occurs at 40°C, is absent in 68 mM KCl resealed ghosts and at lower salt concentrations. Interestingly these membranes maintain both the 8°C and the 20°C transitions virtually unmodified (Fig. 7). As expected, the plot of log (h_0/h_{-1}) vs 1/T for the freely diffusible spin label 16-DSA added to skeletal protein preparations did not detect a thermotropic break at 40°C and spectra were shaped as for a free spin label (data not shown).

DISCUSSION

The data reported in this paper show that the use of spin labeling techniques to study unmodified RBC membrane allows the identification of reproducible thermo-

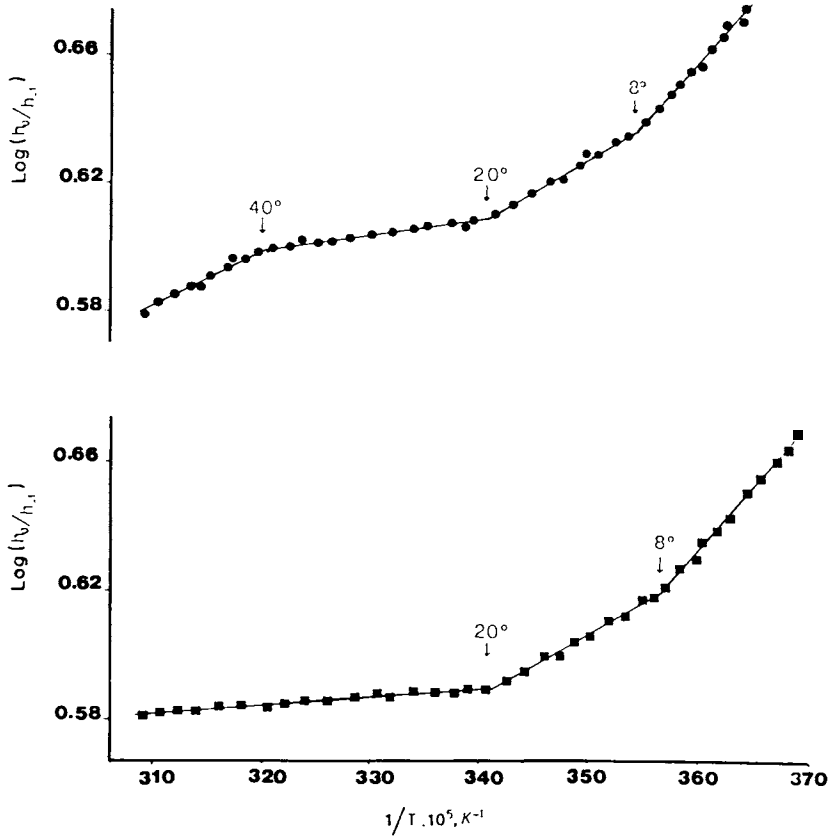

Fig. 7. The plot of log (h_0/h_{-1}) vs 1/T of 16-DSA spin probe for 0.15 M KCl resealed ghosts (●—●) and for 0.068 M KCl resealed ghosts (■—■).

tropic breaks at 8, 20, and 40°C. The observation throughout this work that the temperatures of thermotropic breaks do not randomly change after biochemical membrane treatments seems to rule out the presence of artifacts due to the choice of the empirical parameter log (h_0/h_{-1}). Additional evidence for the presence in RBC of structural transitions at these temperatures can be derived from 1) the observation of similar temperatures in the thermotropic transitions detected by unperturbing spectroscopic techniques [10,18,20,51], 2) data obtained with different spin labels possibly experiencing different motions but showing similar thermotropic breaks [13], 3) data obtained with different spectroscopic techniques employing different probes [23,24,26], and 4) the presence of thermotropic discontinuities at about the same temperatures in some RBC membrane functions [see references 1,3,17,25,31–34 of the accompanying paper, 15].

Before discussing in more detail each thermotropic break detected by 16-DSA, some general problems must be taken into consideration. Owing to membrane anisotropy, the meaning of structural transitions detected in RBC by freely diffusible spin probes are unclear mainly because 1) the involved membrane components and the physical changes responsible for thermotropic breaks are unknown, 2) the time scale of EPR is relatively short ($\sim 10^{-8}$ s) so that the structural transitions may or may not

be due to phase transitions of membrane domains, and 3) stearic acid spin labels may localize in more than one site into RBC membrane. Results suggesting more than one binding site for stearic acid spin labels in RBC membrane have been reported [19,52].

The identification of physical changes involved in the thermotropic transitions is made more difficult by conflicting data obtained with different spectroscopic techniques. Fluorescence and Raman spectroscopies, the time scale of which is shorter than EPR, show the presence of multiple structural transitions in RBC [18,20,23,30]. Techniques with a time scale longer than EPR (10^{-4}–10^{-5}s vs 10^{-8} s, respectively) such as ^{2}H and ^{31}P NMR did not detect thermotropic transitions at $T \geqq -5°C$ in intact RBC [21,31]. Therefore techniques with a short time scale apparently detect thermotropic transitions unobserved by NMR; however, NMR results seem to preclude the existence of thermotropic changes in long-lived membrane domains. Nevertheless the existence of domains, which may possibly occur at a microscopic scale, detected by EPR techniques but undetected by ^{2}H NMR cannot be completely ruled out. In this hypothesis thermotropic breaks detected by lipidic spin labels may be due to thermotropic lateral phase separation processes. For example, measurements of the width of ^{31}P NMR resonance show the presence of an immobilized phospholipid component in membranes recombined with intrinsic RBC proteins [53] and reveal a thermotropic transition at 20°C after neutral lipid extraction and enzymatic digestion of periferal proteins [21]. Interestingly, after chymotrypsin treatment we reported by EPR the presence of only one transition attributed to lipids at the same temperature (Fig. 2). The special sensitivity of spin labels to lipid lateral phase separation [54] supports this hypothesis.

Discrepancies on the effects of intrinsic proteins on lipid order in model membranes have been likewise reported by using different spectroscopic techniques, although they seem to be reconciled in recent papers [55, and references reported therein]. Briefly proteins seem to contribute to lipid order in two ways: a "fast" protein ordering effect on boundary lipids (monitored by spectroscopic techniques with a short time scale), and a "slow" disordering effect on bulk lipids (monitored by ^{2}H NMR). "Ordered" lipids exchange very rapidly with other lipids as ^{2}H NMR results preclude the presence of a long-lived shell around proteins. If intrinsic RBC proteins produce this kind of ordered lipids, the possibility of thermotropic transitions due to these lipids should be considered.

The last possibility is that EPR thermotropic breaks are due to conformational changes of proteins. In this case thermotropic breaks detected by a freely diffusible spin label may represent the protein conformational changes monitored at the level of protein-lipid boundaries or reflected within the membrane as a change in its physicochemical properties (ie, fluidity, lateral mobility of membrane proteins, etc).

A rational approach to these problems may consist of the identification of membrane components possibly involved in these transitions, which is the object of this work. In addition, to overcome the problems of different probe localization, a comparison between different spin labeling techniques may be useful. For example, maleimide spin labels detect a thermotropic transition at 40°C due to spectrin conformational changes [47]. Our experimental results do not support the idea that the break at 40°C of 16-DSA is due to a probe localization into a hydrophobic spectrin pocket where the probe would detect the same conformational changes of maleimide spin label. We observed, in fact, that change of spectrin monitored by maleimide spin label is not abolished in 68 mM KCl resealed ghosts at variance of the 40°C break of

16-DSA (Fig. 7). The transition detected by 16-DSA seems to be affected by the association of skeletal proteins with the membrane. In fact, we do not observe the 40°C transition either in skeleton-free membranes (Fig. 6) or at low salt concentrations.

The transitions detected by lipidic and covalently bound spin labels at 40°C appear to be derived from different membrane domains, although they seem to be dependent by the same membrane component (ie, RBC skeleton). The rapid increase in 16-DSA freedom of motion observed above 40°C (Fig. 2), may be due to a decreased skeleton-membrane interaction. These, in fact, are known to modulate lateral mobility of intrinsic proteins [56]. Moreover, the rotational diffusion of the intrinsic protein band 3 is markedly increased above 40°C [57].

The 20°C transition is preserved after chymotrypsin digestion (Fig. 2) and is lowered to 15°C in protein-free membranes (Fig. 4). These results suggest that this transition may be determined by a lipid thermotropic property modified by the presence of intrinsic proteins.

The 8°C transition is affected by chymotrypsin treatment at the cytoplasmic membrane layer (Figs. 2, 6) and by membrane treatments including the cross-linker glutaraldehyde (Fig. 6 of the accompanying paper [15]). Possible candidates to this transition are the cytoplasmic part of intrinsic proteins or some unidentified components migrating in the zone of bands 4–5. The electrophoretic profile of glutaraldehyde-treated RBC shows, in fact, a strong decrease of polypeptides migrating in this zone (Fig. 5). Owing to the uncertainties on membrane components involved in the 8°C transition one may only speculate on both probe localization and possible structural changes associated with this transition. In this respect a protein-induced lateral phase separation, as we suggested before [14], is a likely hypothesis.

In conclusion, the identification of membrane components involved in RBC thermotropic structural transitions, as preliminarily attempted in this work, may be useful to understand thermotropic membrane phenomena. In addition, molecular defects of pathological membranes with altered thermotropic properties [25,58] may be successfully investigated with this approach.

ACKNOWLEDGMENTS

We thank Drs. G.B. Rossi and G. D'Agnolo for helpful discussions and critical reading of the manuscript. We are indebted to C.M. Cortellessa who performed statistical analyses. We are also grateful to G. Scorza for excellent technical assistance.

This work was partially supported by grant 83.02772.56 from Consiglio Nazionale delle Ricerche, Progetto Finalizzato "Medicina Preventiva e Riabilitativa".

REFERENCES

1. Friend DS: J Cell Biol 93:243–249, 1982.
2. Bretscher MS, Raff MC: Nature 258:43–49, 1975.
3. Op den Kamp JAF: Ann Rev Biochem 48:47–71, 1979.
4. Van Deenen LLM: FEBS Lett 123:3–15, 1981.
5. Demel RA, Jansen JWC, Van Dijck PWM, Van Deenen LLM: Biochim Biophys Acta 465:1–10, 1977.
6. Lange Y, D'Alessandro JS: J Supramol Struct 8: 391–397, 1978.
7. Cullis PR, Van Dijck PWM, De Gier J: Biochim Biophys Acta 513:21–30, 1978.

8. Marinetti GV: Biochim Biophys Acta 465:198–209, 1977.
9. Marinetti GV, Crain RC: J Supramol Struct 8:191–213, 1978.
10. Hui SW, Stewart CM, Carpenter MP, Stewart TP: J Cell Biol 85:283–291, 1980.
11. Zimmer G, Schirmer H, Bastian P: Biochim Biophys Acta 401:244–255, 1975.
12. Weltzien HU, Arnold B, Kalkoff HG: Biochim Biophys Acta 455:56–65, 1976.
13. Tanaka KI, Ohnishi SI: Biochim Biophys Acta 426:218–231, 1976.
14. Minetti M, Ceccarini M: J Cell Biochem 19:59–75, 1982.
15. Minetti M, Ceccarini M, Di Stasi AMM: J Cell Biochem 25:000–000, 1984.
16. Zimmer G, Schirmer H: Biochim Biophys Acta 345:314–320, 1974.
17. Bieri VG, Wallach DFH: Biochim Biophys Acta 406:415–423, 1975.
18. Verma SP, Wallach DFH: Proc Natl Acad Sci USA 73:3558–3561, 1976.
19. Bieri VG, Wallach DFH: Biochim Biophys Acta 443:198–205, 1976.
20. Verma SP, Wallach DFH: Biochim Biophys Acta 436:307–318, 1976.
21. Cullis PR, Grathwohl C: Biochim Biophys Acta 471:213–226, 1977.
22. Sato B, Nishikida K, Samuels TL, Tyler FH: J Clin Invest 61:251–259, 1978.
23. Chernitskii YA, Vorobei AV, Konev SV: Biophysics 23:78–82, 1978.
24. Kapitza HG, Sackmann E: Biochim Biophys Acta 595:56–64, 1980.
25. Laurent M, Daveloose D, Leterrier F, Fischer S, Shapira G: Clin Chim Acta 105:183–259, 1980.
26. Galla HJ, Luisetti J: Biochim Biophys Acta 596:108–117, 1980.
27. Ogiso T, Iwaki M, Mori K: Biochim Biophys Acta 649:325–335, 1981.
28. Janoff AS, Mazorow DL, Coughlin RT, Bowdler AJ, Haug A, McGroarty EJ: Am J Hematol 10:171–179, 1981.
29. Herrmann A, Arnold K, Lassman G, Glaser R: Acta Biol Med Germ 41:289–298, 1982.
30. Verma SP, Wallach DFH: Biophys J 37:155A, 1982.
31. Maraviglia B, Davis JH, Bloom M, Westerman J, Wirtz KWA: Biochim Biophys Acta 686:137–140, 1982.
32. Steck TL, Kant JA: Meth Enzymol 31:172–180, 1974.
33. Gerritsen WJ, Verklej AJ, Van Deenen LLM: Biochim Biophys Acta 555:26–41, 1979.
34. Roelofsen B, Zwaal RFA, Woodward CB: Meth Enzymol 32:131–140, 1974.
35. Laemmli UK: Nature 227:680–685, 1970.
36. Schreier S, Polnaszek CF, Smith ICP: Biochim Biophys Acta 515:395–436, 1978.
37. Shiga T, Maeda N, Suda T, Kon K, Sekiya M: Biochim Biophys Acta 553:84–95, 1979.
38. Tomaselli MB, John KM, Lux SE: Proc Natl Acad Sci USA 78:1911–1915, 1981.
39. Weinstein RS, Khodadad JK, Steck TL: J Supramol Struct 8:325–335, 1978.
40. Steck TL: J Cell Biol 62:1–19, 1974.
41. Nakao M, Nakao T, Yamazoe S: Nature 187:945–946, 1960.
42. Feo CJ, Leblond PF: Blood 44:639–647, 1974.
43. Lutz HU, Liu SC, Palek J: J Cell Biol 73:548–560, 1977.
44. Lutz HU: J Supramol Struct 8:375–389, 1978.
45. Steck TL, Yu J: J Supramol Struct 1:220–232, 1973.
46. Steck TL: J Mol Biol 66:295–305, 1972.
47. Cassoly R, Daveloose D, Leterrier F: Biochim Biophys Acta 601:478–489, 1980.
48. Yamaguchi T, Koga M, Takehara H, Kimoto E: FEBS Lett 141:53–55, 1982.
49. Barber MJ, Rosen GM, Rauckman EJ: Biochim Biophys Acta 732:126–132, 1983.
50. Kozlova NM, Slobozhanina YI, Vorobei AV, Chernitskii YA: Biophysics 24:1142–1144, 1979.
51. Chow EI, Chuang SY, Tseng PK: Biochim Biophys Acta 646:356–359, 1981.
52. Shiga T, Suda T, Maeda N: Biochim Biophys Acta 466:231–244, 1977.
53. Yeagle PL: Biophys J 37:227–239, 1982.
54. Shimshick EJ, McConnel HM: Biochemistry 12:2351–2359, 1973.
55. Jähnig F, Vogel H, Best L: Biochemistry 21:6790–6798, 1982.
56. Smith DK, Palek J: Nature 297:424–425, 1982.
57. Nigg EA, Cherry RJ: Biochemistry 18:3457–3465, 1979.
58. Zarcowsky HS, Mohandas N, Speaker CB, Shohet SB: Br J Haematol 29:537–543, 1975.